

# Cerium moment collapse in ternary silicides $\text{CePd}_{2-x}\text{Mn}_x\text{Si}_2$ ( $0 \leq x \leq 2$ )

Bernhard Rupp

Lawrence Livermore National Laboratory, University of California, Livermore, California 94551

(Received 3 December 1993)

Cerium  $L_3$  XANES (x-ray-absorption near-edge-structure) spectra were analyzed to separate Ce moment contributions and mixed valence (MV) in complex magnetic silicides  $\text{CePd}_{2-x}\text{Mn}_x\text{Si}_2$  ( $0 \leq x \leq 2$ ). The Ce valence mixing does not vary linearly with  $x$ , but increases rapidly for  $x \geq 1.5$ . The associated moment collapse correlates with pronounced deviations of the unit-cell volume from Vegard law and the onset of structural instability. Reorientation of  $[001]$  Mn  $3d$  antiferromagnetic order for  $x < 2$  appears to rapidly suppress the weak Ce valence mixing coexisting with antiferromagnetic order in  $\text{CeMn}_2\text{Si}_2$ .

## I. INTRODUCTION

In a previous study we have reported<sup>1</sup> specific-heat, resistivity, and magnetic properties of  $\text{ThCr}_2\text{Si}_2$ -type alloys  $\text{CePd}_{2-x}\text{Mn}_x\text{Si}_2$  ( $0 \leq x \leq 2$ ). The magnetic phase diagram of the  $\text{CePd}_{2-x}\text{Mn}_x\text{Si}_2$  system consists of different regions of magnetic interactions, and it is briefly reviewed as follows: On the Pd-rich side, the Ce  $4f$   $[110]$  low-temperature antiferromagnetism of the boundary compound  $\text{CePd}_2\text{Si}_2$  becomes slightly enhanced with increasing Mn substitution; on the Mn-rich side, the Mn  $3d$   $[001]$  antiferromagnetic (afm) order becomes rapidly suppressed with increasing Pd substitution. In the intermediate region around  $x \approx 1-1.2$  unresolved low-temperature magnetic order occurs. Strong enhancement of the specific-heat coefficients,  $\gamma$ , in the intermediate region indicated spin fluctuations, and Kondo behavior was inferred. In addition to a change in the moment orientation, which appears to induce a high degree of magnetic frustration associated with the onset of structural instability, the formal valence of Ce in this alloy system, in fact, must change from  $\text{Ce}^{3+}$  in the Pd-rich boundary compound  $\text{CePd}_2\text{Si}_2$  to  $\text{Ce}^{4+}$  in  $\text{CeMn}_2\text{Si}_2$ .  $\text{CeMn}_2\text{Si}_2$  itself is of interest as it displays low-energy valence mixing in coexistence with strong afm  $3d$  magnetic order.<sup>2</sup>

One question which had to remain open in our previous study was to what degree Ce valence mixing exists and how it might correlate with the variations in the magnetic behavior of the alloys. From magnetization measurements alone, one cannot isolate the Ce valence of  $\text{Ce}(\text{Pd,Mn})_2\text{Si}_2$  alloys by Curie-Weiss extrapolation because both the Ce and the Mn magnetic moments contribute the total static susceptibility (see Fig. 4 of Ref. 1). In the present study, we employed cerium  $L_3$  x-ray-absorption near-edge-structure (XANES) spectroscopy to resolve the local Ce moments in the complex magnetic multicomponent system  $\text{CePd}_{2-x}\text{Mn}_x\text{Si}_2$ . XANES spectroscopy also provides additional information on the electronic structure of alloys on the borderline between localized and itinerant behavior.

## II. XANES SPECTROSCOPY

The transition of  $2p_{3/2}$  core level electrons into unoccupied  $nd$  ( $n \leq 3$ ) electronic states results in a "white"

line (peak) at the  $L_3$  absorption threshold. This resonance absorption line is weak or nearly lost in the case of rather itinerant systems such as uranium or in uranium intermetallic alloys<sup>3,4</sup> but prominent in highly localized systems (e.g., oxides). In the case of rare-earth metals, with a high degree of localization of their  $4f$  electrons compared to the  $5f$  electrons in light actinoid elements, even metallic systems exhibit distinct white lines which can be analyzed to explore mixed valence (MV) behavior in rare-earth-transition-metal alloys.<sup>5</sup> Valence mixing or fluctuations occur in systems with  $4f$  (or  $5f$ ) electron levels lying close to the conduction band and lead to a small energy difference between the  $2p_{3/2} \rightarrow 4f^n(5d6s)^m$  and the  $2p_{3/2} \rightarrow 4f^{n-1}(5d6s)^{m+1}$  electronic transitions.<sup>6</sup> In the case of Ce, this second transition is 8–10 eV higher in energy, and gives rise to a second white line, usually appearing as a shoulder or a double-peak feature of the white line at the  $L_3$  absorption threshold. The same is true for  $L_2$ -edge absorption line transitions originating at a  $2p_{1/2}$  ground state.

## III. ANALYSIS OF XANES DATA

XANES spectra are analyzed by deconvoluting them into a Lorentzian line representing the discrete  $2p_{3/2} \rightarrow 4f^n(5d6s)^m$  transition (abbreviated  $f^1$ ) at the threshold resonance and an arctangent function describing the continuum transition.<sup>7</sup> A second Lorentzian represents the  $2p_{3/2} \rightarrow 4f^{n-1}(5d6s)^{m+1}$  transition ( $f^0$ ) to a higher valence level. The spectroscopic mixed valence (SMV) is then derived from the ratio of the components in the ground state:

$$\text{SMV} = 3 + f^0 / (f^1 + f^0). \quad (1)$$

The separation between the absorption threshold region including the white line and the onset of the extended x-ray-absorption fine structure (EXAFS) can be problematic<sup>8</sup> and may lead to difficulties when comparing the XANES of Ce atoms in different structures, where the EXAFS will vary significantly from case to case. In an isostructural series such as  $\text{CePd}_{2-x}\text{Mn}_x\text{Si}_2$ , changes in the nearest-neighbor environment are essentially limited to the electronic effect of the Pd-Mn substitution and to very small distance changes. Their effect on the near-edge structure would be expected to change in correlation

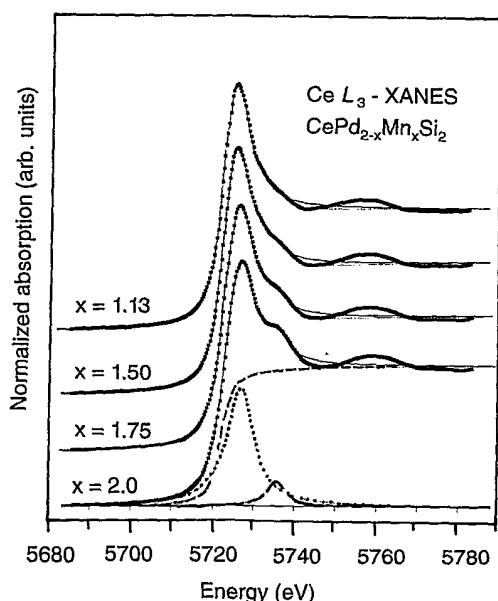


FIG. 1. Ce  $L_3$  XANES spectra of  $\text{CePd}_{2-x}\text{Mn}_x\text{Si}_2$  (293 K) showing a typical deconvolution of the threshold region into two Lorentzian lines corresponding to the respective transitions and the arctangent continuum transition (dashed lines). The resulting fit is shown solid. For  $x < 1.13$  the threshold features look essentially the same and the spectra are omitted.

with the composition. Figure 1 shows that for our sample series, changes in the EXAFS region are very small, and it appears justified to assume that the prominently changing threshold peaks attributed to mixed valence behavior are indeed due to transitions into unfilled  $d$  states. The spectroscopically derived mixed valence is finally correlated in a one-to-one manner to the formal valence: While in cerium-based mixed valence systems the SMV saturates and rarely exceeds a value of 3.3, linear mapping of the SMV to known formal valences derived from lattice constants or magnetic data at the end points of an isostructural series was shown to be justified.<sup>2,4,9,10</sup>

#### IV. EXPERIMENT

Cerium  $L_3$ -edge XANES spectra were recorded on beamline X-11A at the Brookhaven National Synchrotron Light Source. The storage ring was operated at 2.53 GeV with electron beam currents of 120–160 mA. Silicon (111) monochromator crystals were used in combination with entrance slit widths of 0.25 mm providing an energy resolution of about 0.45 eV at 5.6 keV. Powdered sample material was sealed in Kapton tape to prepare transmission foils of uniform thickness corresponding to 1–1.5 absorption lengths. The samples were examined by the conventional transmission technique with an energy scan step size of 0.25 eV. Chromium foil (one absorption length) was simultaneously scanned as an energy reference during each measurement. For details on sample preparation and x-ray analysis refer to a previous study.<sup>1</sup>

#### V. RESULTS AND DISCUSSION

Due to the high spectrometer resolution compared to the  $2p_{3/2}$  core-hole lifetime, it was not necessary to fold the Lorentzian line with a Gaussian (instrumental) broadening term in order to obtain very good white line fits (Fig. 1).  $4f^n-4f^{n+1}$  shakedown satellites<sup>11</sup> were not observed in our spectra. The course of the analysis was straightforward, thus we omit a tabular presentation and summarize as follows: The exciting result is the rapid increase of MV behavior for  $x \geq 1.5$ ; the values analyzed according to formula (1) can be derived from Fig. 2 and a detailed discussion follows below. In addition, we observe a minor upshift in energy for the  $f^0$  peak associated with a 10% increase in peak half width with higher Mn contents. Both effects are consistent with increased formal Ce valence and moment delocalization, but the changes were too small to warrant further analysis.

The valence mixing value of 3.13 obtained for  $\text{CeMn}_2\text{Si}_2$  from our spectra is in perfect agreement with the 3.12 independently reported by Liang *et al.*<sup>2</sup> and underscores the reproducibility of the analysis. Figure 2 allows us to correlate the valence mixing with changes in the antiferromagnetic ordering temperature and cell volume which were already reported in a previous study.<sup>1</sup>

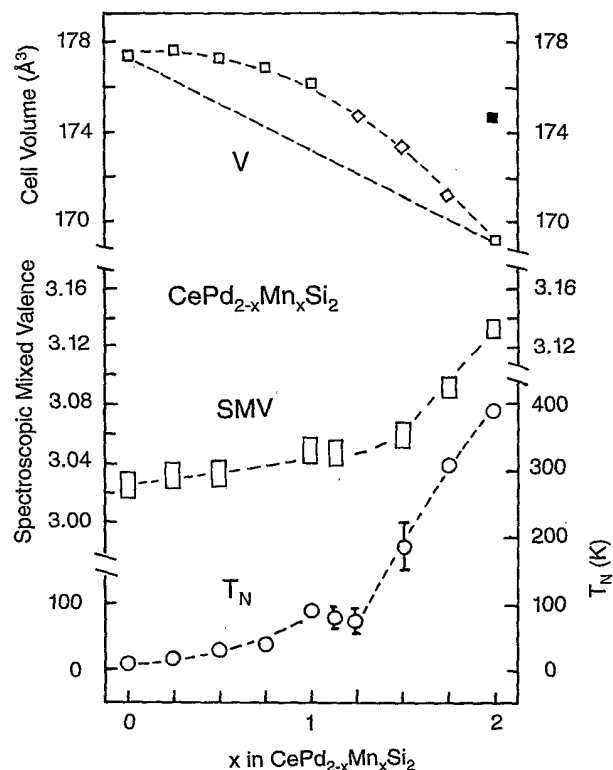


FIG. 2. Variation of unit-cell volume ( $V$ ), valence mixing (SMV), and antiferromagnetic transition temperature ( $T_N$ ) vs Pd-Mn substitution in  $\text{CePd}_{2-x}\text{Mn}_x\text{Si}_2$ . If not explicitly depicted, the size of the symbols reflects the corresponding error estimates. Dashed lines are guides to the eye only. Open squares denote tetragonal  $\text{ThCr}_2\text{Si}_2$  structure type, open diamonds a orthorhombic distortion. The solid square represents an estimated value for  $\text{Ce}^{(\text{III})}\text{Mn}_2\text{Si}_2$ . For a detailed explanation we refer to the discussion section.

It is evident from Fig. 2 that the regions of moment collapse and structural instability coincide. We have estimated a cell volume (depicted as a solid square in Fig. 2) for  $\text{Ce}^{(\text{III})}\text{Mn}_2\text{Si}_2$  on the basis of  $\text{Ce}^{(\text{III})}/\text{Ce}^{(\text{IV})}$  radius ratio assuming an actual formal valence of  $4+$  in  $\text{CeMn}_2\text{Si}_2$ . In a first approximation, allowing a straight extrapolation from  $\text{Ce}^{(\text{III})}\text{Pd}_2\text{Si}_2$  to  $\text{Ce}^{(\text{III})}\text{Mn}_2\text{Si}_2$ , one can very well associate the onset of cell volume decrease and structural instability for  $x \geq 1.5$  with the Ce moment collapse.

An interpretation of the enhanced valence mixing and the magnetic order for  $x \geq 1.5$  can be attempted in the framework suggested by Liang *et al.*<sup>2</sup> and our previous work.<sup>1</sup> The argument has been made that the position of the Ce atoms symmetrically sandwiched between antialigned ferromagnetic layers of Mn puts the Ce atoms at nodes of the internal field,<sup>2</sup> thus leaving the weak MV interactions essentially undisturbed. A reorientation of the spin axis by Mn-Pd substitution, beginning at the already low Pd values suggested earlier,<sup>1</sup> would consequently remove this condition and expose the Ce sites to an internal field rapidly suppressing the mixed valence character upon further Mn-Pd substitution.

For the intermediate region  $0.5 \leq x \leq 1.2$ , which is characterized by strong  $\gamma$  enhancement and spin reorientation in combination with presumably  $3d$ -enhanced

low-temperature afm Ce order,<sup>1</sup> the Ce valence mixing remains small but stable. Apparently no obvious correlation between low-temperature  $\gamma$  enhancement, spin-flip behavior, and the normal-state (room-temperature) Ce valence mixing exists. We wish to reemphasize that the moment reorientation occurring in this region must be complex and not a conventional type. A closer look at the temperature dependence of the Ce valence mixing covering the critical regions might be of interest, but is currently beyond our means.

In view of the nonlinear valence variation established in this study, one of our earlier extrapolations based on the assumption of a linear change of the Ce moment over the whole series can be refined: Allowing one-to-one mapping of the SMV to the observed formal valence-moment of Ce in our alloys, we extrapolate a magnetic moment for Mn in infinite dilution of  $4.2$  instead of  $5.6\mu_B$ .

#### ACKNOWLEDGMENTS

This work was supported by the United States Department of Energy at LLNL under Contract No. W-7405-ENG-48. Samples were prepared at the University of Vienna by Peter Rogl and B.R. under Grant No. P5279 of the Austrian Science Foundation (FWF).

- <sup>1</sup>B. Rupp, P. Rogl, N. Pillmayr, G. Hilscher, and G. Schaudy, *Phys. Rev. B* **41**, 9315 (1990).
- <sup>2</sup>G. Liang, I. Perez, D. DiMarzio, M. Croft, D. C. Johnston, N. Anbalagan, and T. Mihalisin, *Phys. Rev. B* **37**, 5970 (1988).
- <sup>3</sup>G. Kalkowski, G. Kaindl, W. D. Brewer, and W. Krone, *Phys. Rev. B* **35**, 2667 (1987).
- <sup>4</sup>G. Kalkowski, G. Kaindl, S. Bertram, G. Schmiester, J. Rebizant, J. C. Spirlet, and O. Vogt, *Solid State Commun.* **64**, 193 (1987).
- <sup>5</sup>R. A. Neifeld, M. Croft, T. Mihalisin, C. U. Segre, M. Madigan, M. S. Torikachvili, M. B. Maple, and L. E. DeLong, *Phys. Rev. B* **32**, 6928 (1985).
- <sup>6</sup>J. M. Lawrence, M. L. den Boer, R. D. Parks, and J. L. Smith, *Phys. Rev. B* **29**, 568 (1984).

- <sup>7</sup>J. A. Horsley, *J. Chem. Phys.* **76**, 1451 (1982).
- <sup>8</sup>Lytle and Gregor [F. W. Lytle and R. B. Gregor, *Appl. Phys. Lett.* **56**, 192 (1990)] have suggested matching the  $\pi$  phase-shifted  $L_1$  EXAFS (which originates from an  $s$  to continuum transition and therefore does not contain a discrete preedge transition) with the  $L_3$ -edge EXAFS. In our case, the low intensity of the  $L_1$  spectra did not allow us to apply their procedure.
- <sup>9</sup>R. D. Parks, S. Raen, M. L. denBoer, V. Murgai, and T. Mihalisin, *Phys. Rev. B* **28**, 3556 (1983).
- <sup>10</sup>M. Croft, R. Meifield, C. U. Segre, R. D. Parks, and S. Raen, *Phys. Rev. B* **30**, 4164 (1984).
- <sup>11</sup>S. Raen and R. D. Parks, *J. Magn. Magn. Mater.* **47**, 200 (1985).